Chemical Physics 81 (1983) 263–271
North-Holland Publishing Company

THE LOWER ELECTRONIC STATES OF MoN

Janet N. ALLISON [1] and William A. GODDARD III

Arthur Amos Noyes Laboratory of Chemical Physics [2], California Institute of Technology, Pasadena, California 91125, USA

Received 20 June 1983

We find that the ground state of MoN($^4\Sigma^-$) has a covalent triple bond where the σ bond is d_{z^2}-like on the Mo, leading to a quartet state with unpaired electrons in the Mo 5s, Mo $4d\delta_{xy}$, and Mo $4d\delta_{x^2-y^2}$ orbitals. The first excited state ($^4\Pi$) corresponds to the $5p\pi \leftarrow 5s$ excitation. The calculated properties of $R_e = 1.60$ Å, $\omega_e = 1100$ cm^{-1}, $D_e = 4.07$ eV, and ΔE ($^4\Pi - {}^4\Sigma^-$) = 2.128 eV are in good agreement with recent experimental results ($R_e = 1.63$ Å and $\Delta E = 2.011$ eV). Particularly interesting is a dramatic non-monotonic change of dipole moment with distance ($\mu = -3.123$ D at $R_e = 1.60$ Å, -5.982 D at $R = 2.60$ Å and $\mu = -0.176$ D at $R = 5.0$ Å). This effect is explained.

1. Introduction

A number of systems with double and triple M–C and M–O bonds (where M is a transition metal) have now been characterized experimentally [1] and theoretically [2] and have been shown to play a role in catalytic reactions [1–3]. Although M–N double and triple bonds are believed to play a role in some catalytic processes (e.g., Mo=NR and Mo≡N in nitrogenase [4] and Mo=NR in ammoxidation catalysts [5]), few such cases have been studied experimentally or theoretically. On the experimental side, Dunn and co-workers [6] have examined the spectra of a number of transition metal nitrides, one of which is Mo≡N. As part of a project to examine the role of Mo–N moieties in catalytic reactions, we have examined the ground and excited states of Mo≡N and compared the results with current experimental data.

2. Character of the Mo≡N bond

Mo has an s^1d^5 ground state with six electrons in separate orbitals, while N has an s^2p^3 ground

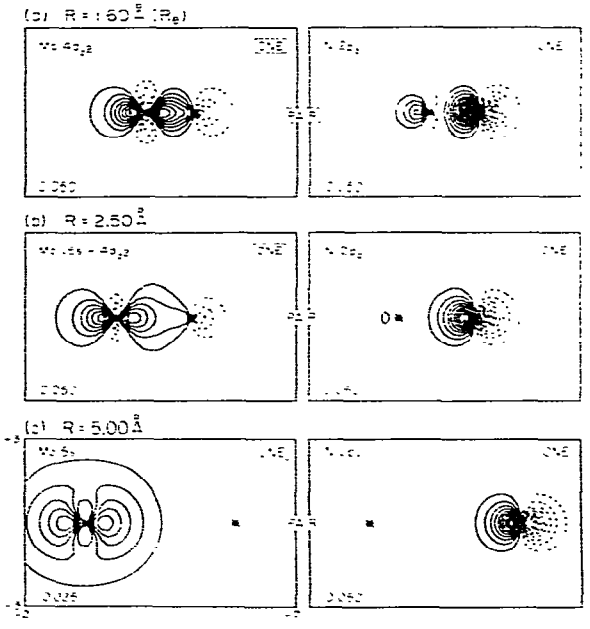

Fig. 1. GVB orbitals for the σ bond of MoN($^4\Sigma^-$) as a function of internuclear distance. Note the conversion of Mo $4d_{z^2}$-like orbital at 1.60 Å (R_e) to an Mo 5s-like orbital at $R = 5.00$ Å. Contour increments (au) noted in the lower left-hand corner. Solid lines indicate positive contours and dashed lines negative contours; the nodal lines are not shown.

[1] Fannie and John Hertz Foundation Predoctoral Fellow.
[2] Contribution No. 6861.

0301-0104/83/0000-0000/S03.00

state with electrons in three separate p orbitals. Thus we expect a triple bond (σ, π_x, π_y) with the Mo retaining three unpaired electrons ($\delta_{x^2-y^2}$, δ_{xy}, and σ) leading to a $^4\Sigma^-$ state. An important question is whether the Mo part of the σ bond involves the 5s orbital, the 4d orbital, or some hybrid combination. As indicated in fig. 1, we find indeed that at large R (5.0 Å) the σ-bond involves a nearly pure 5s orbital but that the character changes rapidly to 4d-like at 2.5 Å and remains 4d-like at R_e (1.60 Å). At R_e the triple bond is highly covalent and involves Mo d-like orbitals in all three bonds (see figs. 1 and 2). This leaves the two dδ orbitals and a 5s-like orbital for three non-bonding valence electrons. This non-binding σ orbital is shown in fig. 3 where we see that it changes from $4d_{z^2}$-like at large R to 5s-like at R_e.

Because of the disparity between the sizes of the $4d_{z^2}$ and 5s orbitals, plots of contours with equal amplitude spacing lead to numerous contours for $4d_{z^2}$ but few for 5s, providing the illusion of 4d character in an orbital that is mainly 5s. In order

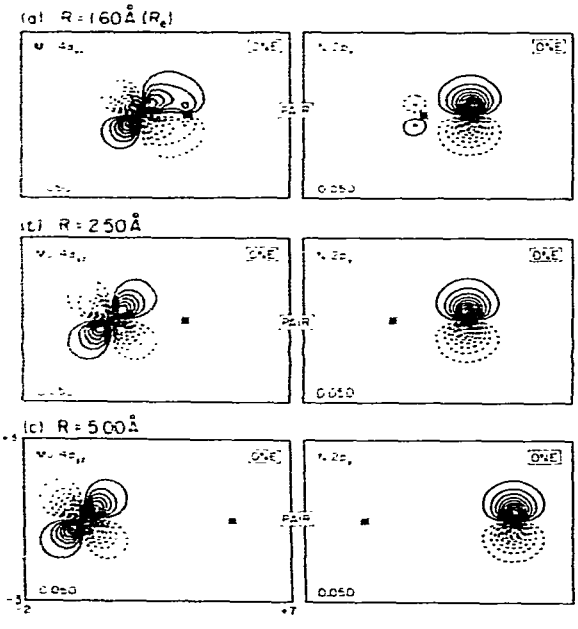

Fig. 2. GVB orbitals for the π bond of MoN($^4\Sigma^-$) as a function of internuclear distance.

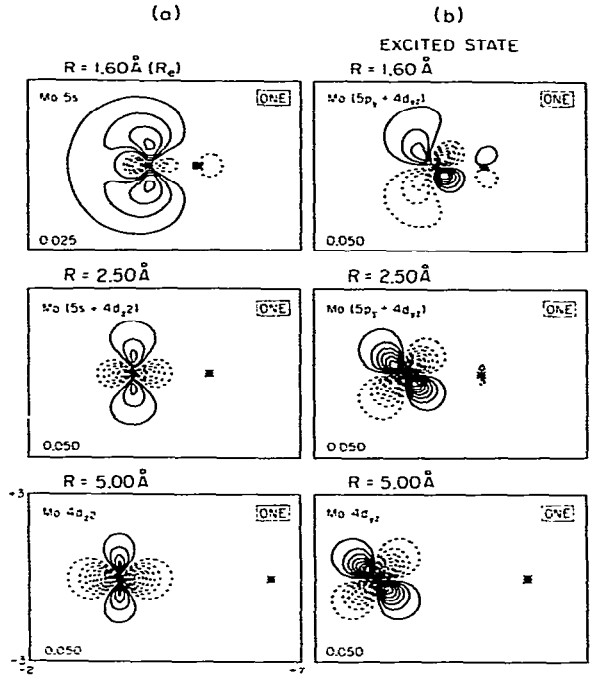

Fig. 3. (a) Singly occupied σ non-bonded orbital of MoN($^4\Sigma^-$) as a function of internuclear distance. Note the conversion of the diffuse Mo 5s-like orbital at $R = 1.60$ Å (R_e) to an Mo $4d_{z^2}$-like orbital at $R = 5.00$ Å. (b) Singly occupied MoN($^4\Pi$) π non-bonded orbital as a function of internuclear distance. Note the increasing Mo $4d_{xz}$ character as R is increased.

to help display the full character of orbitals with 5s character, several of the plots in figs. 1 and 3 contain contours at 0.0250 au spacing rather than 0.050 au spacing, as indicated in the lower left portion of each figure.

In order to provide a more quantitative description of the atomic character of these orbitals, we have calculated Mulliken populations for the MoN σ bond and for the Mo σ non-bonded, singly occupied orbital of the full GVB wavefunction. These results are shown in table 1 and fig. 4. At R_e, GVB calculations indicate there are 0.76 Mo d electrons in the σ bond, which decreases to 0.04 Mo d electrons at $R = 5.00$ Å. As the d character *decreases* in the σ bond, the d character *increases* in the singly occupied Mo σ non-bonded Mo orbital (from 0.10 *e* at $R_e = 1.6$ Å to 0.94 *e* at $R = 5.0$ Å).

Table 1
Mulliken populations for the GVB orbitals of MoN($^4\Sigma^-$)

σ-bond (two-electron total)				Non-bonded σ orbital (one-electron total)		
R (Å)	Mo d	Mo sp	N spd	Mo d	Mo sp	N spd
the full GVB wavefunction (GVB-3)						
1.60	0.76	0.04	1.20	0.10	0.87	0.03
2.00	0.60	0.12	1.28	0.22	0.77	0.01
2.50	0.44	0.34	1.22	0.47	0.53	0.00
3.00	0.34	0.56	1.10	0.64	0.36	0.00
5.00	0.04	0.96	1.00	0.94	0.06	0.00
the GVB PP wavefunction						
1.60	0.75	0.05	1.20	0.12	0.84	0.04
2.00	0.48	0.14	1.38	0.29	0.69	0.02
2.50	0.30	0.30	1.40	0.51	0.49	0.00
3.00	0.24	0.50	1.26	0.67	0.33	0.00
5.00	0.04	0.96	1.00	0.96	0.04	0.00

In fig. 4 we see that at $R = 2.47$ Å the number of electrons in the σ bond is equal to the number in the non-bonding orbital. In the sections 3 and 4 we will find that the total dipole moment is a maximum at this point.

From fig. 4 we see that the *total number* of Mo d electrons in the σ bond plus Mo non-bonding orbital is essentially unity for $R > 3.0$ Å but drops to 0.80 near R_e.

The reason for the change in character of the σ bond is as follows. The exchange energy for Mo(^{7}S) in the s^1d^5 configuration is

$$E^{ex} = -10K_{dd} - 5K_{sd}.$$

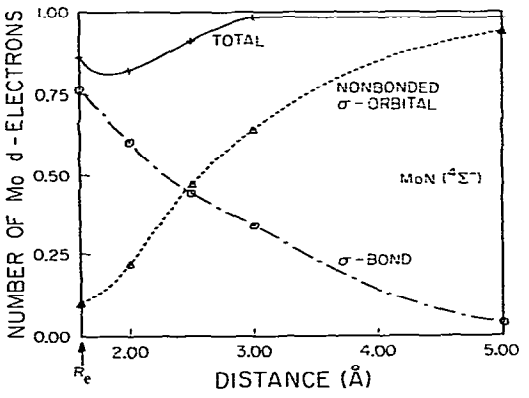

Fig. 4. Number of Mo d electrons for the Mo σ non-bonded orbital and the MoN σ bond.

where *

$K_{dd} = 0.540$ eV, $K_{sd} = 0.306$ eV.

If the s orbital is used in a perfect valence bond to another atom, the exchange energy becomes

$$E^{ex}(\text{s bond}) = -10K_{dd} - \tfrac{5}{2}K_{sd}.$$

and the bond energy can be written as

$$D(\text{s bond}) = D_s - \tfrac{5}{2}K_{sd} = D_s - 0.765 \text{ eV},$$

where D_s is the bond strength ignoring exchange terms.

If, instead, a d orbital is used in a perfect valence bond to another atom, the exchange energy becomes

$$E^{ex}(\text{d bond}) = -8K_{dd} - \tfrac{9}{2}K_{sd}.$$

and the bond energy will be written as

$$D(\text{d bond}) = D_d - 2K_{dd} - \tfrac{1}{2}K_{sd} = D_d - 1.233 \text{ eV}.$$

Thus, at large distances where D_s and D_d are both small, the exchange terms favor bonding to the s orbital. On the other hand, for short R, the intrinsic bond strength (D_d) is much larger for a d orbital (D_d) than for an s orbital (D_s), as an s orbital has much lower contragradience [7]. Thus, for small distances, increased d character in the

* Based on all-electron ab initio calculations.

bond is favored. This trend is aided by the two π bonds. Thus the exchange interaction for one sσ bond and two 4dπ bonds is

$$E^{ex}(s\sigma,\pi_x,\pi_y) = -\tfrac{13}{2}K_{dd} - \tfrac{5}{2}K_{sd},$$

while for one dσ bond and two 4dπ bonds it is

$$E^{ex}(d\sigma,\pi_x,\pi_y) = -\tfrac{11}{2}K_{dd} - \tfrac{7}{2}K_{sd}$$

leading to

$$D(s\sigma,d\pi,d\pi) = D_{s\sigma} + 2D_{d\pi} - \tfrac{7}{2}K_{dd} - \tfrac{5}{2}K_{sd}$$
$$= D_{s\sigma} + 2D_{\pi} - 2.655 \text{ eV},$$
$$D(d\sigma,d\pi,d\pi) = D_{d\sigma} + 2D_{d\pi} - \tfrac{9}{2}K_{dd} - \tfrac{3}{2}K_{sd}$$
$$= D_{d\sigma} + 2D_{\pi} - 2.889 \text{ eV}.$$

Thus, because of the π bonds, the loss in exchange stabilization due to a dσ bond is reduced, leading to increased d character in the bond. These factors explain the overall character of fig. 4.

3. Dipole moment of MoN($^4\Sigma^-$)

In fig. 5 we show the dipole moment (solid line) for $^4\Sigma^-$ MoN. At R_e the dipole moment is large (-3.123 debye $= -1.229$ au) and negative (corresponding to Mo^+N^-). In a point-charge model this dipole moment would correspond to a charge transfer of 0.41 electrons from Mo to N. Noteworthy here is that the dipole moment does *not* change monotonically with R. Thus the dipole moment is a maximum (-5.982 debye $= -2.353$ au) at $R = 2.60$ Å, a distance 62% larger than R_e.

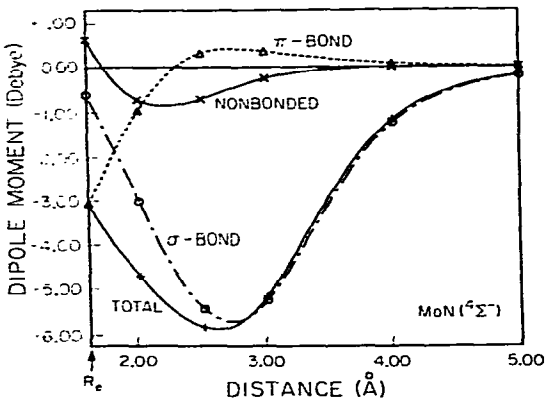

Fig. 5. Dipole moment of MoN($^4\Sigma^-$) as a function of internuclear distance. The four curves represent the π-bond contribution, the σ-bond contribution, the non-bonded contribution, and the overall total dipole moment.

In order to examine the origin of this behavior, we have partitioned the *total dipole* into three parts: the contribution from the Mo non-bonded orbitals plus core orbitals; the contribution from the MoN σ bond; and finally, the contribution from the two π bonds. These results are listed in table 2 and plotted in fig. 5. At $R = 5.0$ Å the various components of the dipole moment are all small. As R is decreased from 5.0 Å, the s character in the σ bond decreases and the d character increases so that by $R = 2.50$ Å an equal amount of s and d character is present (see fig. 4). This is the region in which the magnitude of the total MoN dipole moment is the greatest, -2.353 au (see fig. 5), with the polarity M^+N^-. As R is decreased further, the magnitude of the dipole moment decreases to -3.123 debye (-1.2288 au) at $R_e = 1.60$ Å, still with the polarity Mo^+N^-.

When the bond has Mo s character, there are two factors favoring a dipole moment with sign Mo^-N^+. First, the 5s orbital is easily polarized using the empty 5p orbital to obtain greater overlap with the N, whereas the 4d orbital is more costly to polarize (requiring a 4f-like orbital for maximal polarization). Secondly, the 5s IP (7.10 eV) [8] is much less than the 4d IP (8.56 eV) [8], allowing greater charge transfer. For example, at $R = 2$ Å, the strength of a purely-ionic bond (ignoring overlap effects) would be

$$D_{s\ ion}(\text{eV}) = \text{EA(N)} + 14.4/R(\text{A}) - \text{IP(Mo 5s)}$$
$$= 0.10 \text{ eV},$$
$$D_{d\ ion}(\text{eV}) = \text{EA(N)} + 14.4/R(\text{A}) - \text{IP(Mo 4d)}$$
$$= -1.36 \text{ eV}.$$

for s and d bonds, respectively. This indicates that charge transfer will be important if the bond has Mo s character but not if it has Mo d character. As R decreases from ∞ to 2.6 Å, the charge transfer in the bond increases due to the greater favoring of ionic character (the $1/R$ term) despite the gradual increase in d character. As the bond becomes dominated by the d character for smaller

Table 2
Contributions to the dipole moment (μ) of MoN($^4\Sigma^-$) as a function of internuclear distance (R). Positive μ is for Mo$^+$N$^-$, based on GVB-PP wavefunctions

R (Å)	Contributions (au) [a]			Total dipole (μ)	
	σ-bond	π-bonds (two)	non-bonding orbitals	(au)	(debye)
1.60	−0.2492	−1.2136	−0.2340	1.2288	−3.1233
2.50	−2.1721	0.1224	−0.2860	−2.3357	5.9368
5.00	−0.07544	0.004751	0.001436	−0.06925	0.1760

[a] The dipole moment was partitioned into orbital contributions by calculating the orbital moment and adding the nuclear contribution due to an equal number of protons centered on appropriate centers (one proton on each nucleus for bond pairs).

R, there can be little charge transfer, leading to a dipole moment contribution at small R that is small (−0.64 D). The result then is a Morse-like dipole contribution from the σ bond, with a minimum of −5.98 D at 2.67 Å.

In addition to the above contributions from the σ bond, we find that for $R < 1.8$ Å the π system dominates. This is due to the charge transfer associated with the MoN covalent π bonds at smaller R. Note that for $R > 2.6$ Å the π system responds to the Mo$^-$N$^-$ character in the σ system by donation of Nπ character to the molybdenum (fig. 5).

4. Dipole moment of MoN($^4\Pi$)

Similar non-monotonic behavior regarding the trend of the total dipole moment is also found for the $^4\Pi$ excited state (fig. 6). Just as there is a choice for MoN($^4\Sigma^-$) between bonding an Mo 5s or Mo $4d_{z^2}$ orbital to the N $2p_z$ orbital, there is an analogous situation for the π system for MoN($^4\Pi$) As Mo(^{7}P) and N(^{4}S) are brought together from their atomic limits, there is a choice between bonding an Mo $5p_y$ or Mo $4d_{yz}$ orbital to the N $2p_y$ orbital.

At large distances, the exchange terms favor bonding of the Mo $5p_y$ over Mo $4d_{yz}$ and the IP ($IP_{5p} = 3.89$ eV versus $IP_{4d} = 9.74$ eV) [8] is such that the charge transfer is even larger than for MoN($^4\Sigma^-$). At smaller R, the *larger* covalent bond strength possible for Mo $4d_{yz}$ leads to increased d character and eventually a decrease in the charge transfer. This results in a maximum in the dipole moment of $\mu(3.25\ \text{Å}) = -4.542$ au $= -11.545$ D (see fig. 7) with polarity M$^+$N$^-$ (corresponding to a transfer of 0.75 electrons from Mo to N). As R is decreased from 3.0 Å to $R_e = 1.59$ Å, the magnitude of the dipole decreases to −1.793 au = −4.556 D, still with polarity M$^+$N$^-$. As R is decreased further and approaches 2.0 Å, the π bonding becomes more covalent, involving primarily to Mo $4d_{yz}$ and N $2p_y$ orbitals. The overall

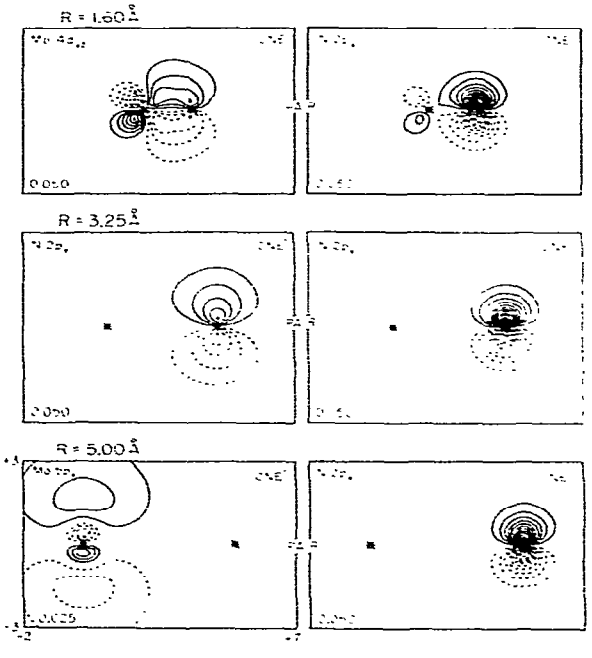

Fig. 6. GVB orbitals for the π bond of MoN($^4\Pi$) as a function of internuclear distance.

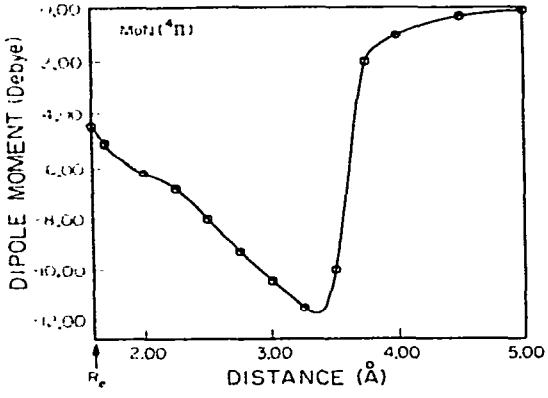

Fig. 7. Total dipole moment of MoN($^4\Pi$) as a function of internuclear distance.

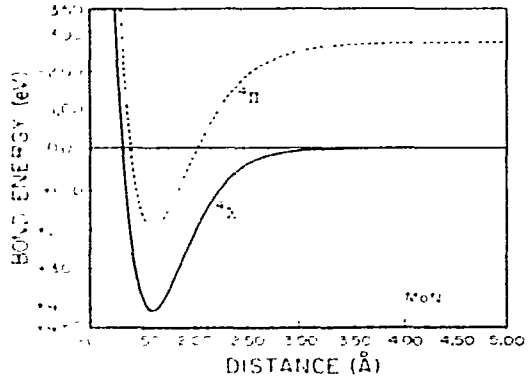

Fig. 8. Potential curves for the ($^4\Sigma^-$) ground state and ($^4\Pi$) excited state of MoN using the full GVB wavefunction. The energy (eV) is relative to Mo(^{7}S) and N(^{4}S) HF atomic limits.

effect is shown by a change in sign of the dipole derivative at $R = 3.25$ Å, which is where the N $2p_\pi$ orbital begins to donate charge *back* to the Mo $4d_{\pi^2}$ orbital.

5. Spectroscopic properties and the excited state

The first excited state of MoN corresponds to excitation of the 5s-like non-bonding orbital into a 5p π-like orbital, leading to a $^4\Pi$ state. The potential energy curves of these states are shown in fig. 8 and the spectroscopic properties tabulated in table 3. We find (see table 3) that removal of the non-bonding σ electron leads to a slightly longer R_e (by 0.005 Å) and a smaller vibrational frequency (by 200 cm^{-1}). The total excitation energy is calculated to be 2.13 eV = 17166 cm^{-1}, which is in good agreement with the experimental value of 2.01 eV = 16217 cm^{-1} [6].

6. Calculational details

Electron correlation is extremely important for a system such as Mo≡N with multiple bonds. Thus, the Hartree–Fock (HF) description gives a bond distance too short by ≈ 0.1 Å and shows MoN to be *unbound* by 0.35 eV (see fig. 9).

Wavefunctions. In order to adequately describe the bonding in MoN, we have carried out calculations using generalized valence bond (GVB) and GVB RCI wavefunctions in which the three pairs

Table 3
Spectroscopic properties for MoN from the full GVB calculation (GVB-3)

State	Total energy (hartree) [c]	Bond dissociation energy D_e (eV)	Bond distance (Å)		Force constant k (hartree/Å^2) [f]	Harmonic vibrational frequency ω_e (cm^{-1})	Excitation energy T_0 (eV)	
			theory R_e	exp. [c] R_0			theory	expt.
$^4\Sigma^-$	−102.773612	4.075 [a]	1.603	1.633	2.0076	1100.4	0	0
$^4\Pi$	−102.695397	4.639 [b]	1.608	1.654	1.3419	899.6	2.116	2.0107 [d]

[a] For MoN($^4\Sigma^-$), the D_e is with respect to (^{7}S) Mo and (^{4}S) N atomic limits.
[b] For MoN($^4\Pi$), the D_e is with respect to (^{7}P) Mo and (^{4}S) N atomic limits.
[c] Calculated from rotational constant B_0 in ref. [6].
[d] See ref. [6].
[e] Calculations on the atoms yield E(Mo) = −48.229487 hartree and E(N) = −54.394390 hartree.
[f] To convert to dynes/cm, multiply by 4.359814×10^5.

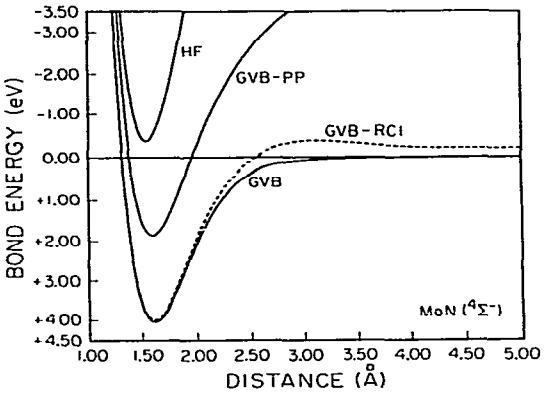

Fig. 9. Potential curves for MoN($^4\Sigma^-$) using HF GVB PP, GVB RCI, and GVB wavefunctions.

of bonding orbitals (one σ and two π) have been correlated. In fig. 9 we show the results of a GVB perfect pairing (GVB PP) calculation leading to a bond dissociation energy D_e of 1.93 eV with respect to the appropriate atomic limits. Using the perfect-pairing restriction, the GVB wavefunction (denoted GVB PP) dissociates properly to the atomic framents but not to the proper spin state [Mo(^{7}S) and N(^{4}S)]. The reason is that the three bond pairs remain singlet-coupled, prohibiting the high-spin coupling of the orbitals on each atom as dissociation occurs.

A common way to solve this problem is to use the *orbitals* from the GVB PP wavefunction but to allow them to be combined so as to describe a general spin-coupling of the electrons. This is accomplished by a small configuration interaction (CI) calculation (referred to as GVB RCI) in which the two electrons of each singlet pair from GVB PP are allowed any occupation of the two orbitals of that pair. In a CI description, the GVB PP wavefunction of MoN($^4\Sigma^-$) would have $2^3 = 8$ configurations, each with three open-shell (unpaired) electrons. In the GVB RCI description, there are $3^3 = 27$ spatial configurations, some of which have up to nine open-shell (unpaired) electrons. The GVB RCI leads to a bond energy of 4.03 eV, a significant improvement over the value of 1.93 eV for GVB PP. (It is important to allow a total of nine open shells (three singly occupied Mo orbitals plus six GVB orbitals involving three bond pairs); thus, if only five open shells are allowed, the calculated D_e is only 2.20 eV.)

Although the GVB RCI gives a quantitatively good description for small R, it dissociates to a limit just slightly above that of the high-spin products. This is because the orbitals (obtained from GVB PP) have incorrect shapes. The result is a small hump in the potential curve (0.36 eV at 3.00 Å). In order to obtain the optimum orbitals *while* including the optimum spin coupling, we use the GVB3 program [9] in which all orbitals are solved for self-consistently for the full 27 configurations of the RCI wavefunction (188 spin eigenfunctions). This corresponds closely to the *full GVB wavefunction* including spin-coupling optimization. As indicated in fig. 9, the GVB wavefunction dissociates monotonically to the Mo(^{7}S) and N(^{4}S) limit. At R_e the full GVB wavefunction leads to a bond energy of 4.075 eV, just slightly better than GVB RCI (4.071 eV). Total energies, the equilibrium internuclear distance, and bond dissociation energies for the various wavefunctions are shown in table 4.

As a final wavefunction, we allowed all single excitations from all occupied orbitals of the 27 GVB RCI configurations to *all* the virtual orbitals (1199 configurations and 10592 spin eigenfunctions). This is referred to as GVB+S (for full GVB

Table 4
Total energies (hartree) for MoN($^4\Sigma^-$) at selected distances

	$R = 1.60$ Å	$R = 5.0$ Å	$R = \infty$	R_e	D_e
HF	−102.604386	−101.832822	−102.623877	1.531	−0.354
GVB PP	−102.694597	−102.460020	−102.623877	1.586	1.930
GVB RCI	−102.371942	−102.617269	−102.623877	1.599	4.029
GVB	−102.773604	−102.623951	−102.623877	1.602	4.075
GVB+S	−102.791694	−102.623870	−102.623877	–	4.566

Table 5
Total energies (au) for MoN($^4\Sigma^-$) and MoN($^4\Pi$) as a function of internuclear distance R(Å) for the full GVB wavefunction

R(Å)	Energy (au)	
	MoN($^4\Sigma^-$)	MoN($^4\Pi$)
1.30	−102.608924	−102.535795
1.50	−102.760771	−102.683865
1.55	−102.770538	−102.692835
1.60	−102.773604	−102.695356
1.65	−102.771565	−102.693954
1.70	−102.765753	−102.688178
1.80	−102.747031	−102.669822
1.90	−102.724136	−102.647518
2.00	−102.701492	−102.625385
2.50	−102.638433	−102.556650
3.00	−102.626591	−102.533309
4.00	−102.624228	−102.525966
5.00	−102.623951	−102.525112

times singles). The result is a bond energy of 4.57 eV.

The spectroscopic properties in table 3 were obtained from the full GVB wavefunction, while dipole moments (table 2 and fig. 5) and orbital plots were derived from GVB PP wavefunctions. Results from table 1 and fig. 4 were obtained from the full GVB wavefunction.

The total energies of MoN($^4\Sigma^-$) and MoN($^4\Pi$) for the full GVB wavefunction at various internuclear distances are tabulated in table 5.

7. Basis set and potential

We have replaced the Zn ($Z = 30$) core of Mo ($Z = 42$) by a relativistic effective potential (Hay [10]) thereby treating Mo as a $(4p)^6(4d)^5(5s)^1$ 12-electron system. The Mo basis consisted of a [3s,4p,2d] contraction basis of a (3s,5p,3d) set of primitive gaussians and is listed in table 6. For

Table 7
Molybdenum relativistic effective potential (Hay [10]). Zinc ($Z = 30$) core

Potential	n	Exponent	Coefficient
V(F)	−2	1372.0024773	−0.0469492
	−1	347.6884970	−22.4419712
	0	109.3720055	−213.5085108
	0	29.8704273	−81.4886889
	0	9.9849325	−32.6181249
	0	3.1672028	−4.6391726
	0	1.1726745	−0.6331185
	0	0.3500768	−0.0379478
V(S−F)	−2	21.0238078	0.9759469
	−1	337.7257282	30.4278849
	0	84.1373438	389.5922948
	0	24.3411662	82.1691652
	0	6.1252823	45.6400558
	0	2.0836763	20.9601999
	0	0.7715966	6.4880764
	0	0.2753636	0.7612272
V(P−F)	−2	20.8605530	1.9683670
	−1	707.9378987	106.2638639
	0	116.6079108	659.3488281
	0	27.8971504	254.1846899
	0	7.7431203	69.6378928
	0	2.2282950	8.5106535
	0	0.5071089	−0.4207005
V(D−F)	−2	13.0268827	2.9811493
	−1	2588.2646370	296.0784376
	0	507.9636789	2831.2924333
	0	97.7322200	450.6802248
	0	20.9699908	72.0312845
	0	5.9597652	27.6522954
	0	2.0768315	4.0536147
	0	0.2284265	−0.0719758

Table 6
Molybdenum basis (Hay [10]). The [3s, 4p, 2d] contracted basis for Mo, $E = -48.229487$ hartree

s basis		p basis		d basis	
α_s	c_s	α_p	c_p	α_d	c_d
0.6748	1.0000	9.6460	−0.05404	2.3540	0.20492
0.07682	1.0000	1.2340	0.64149	0.7053	0.57381
0.02911	1.0000	0.4261	1.0000	0.1865	1.00000
		0.08874	1.0000		
		0.02660	1.0000		

nitrogen, the Dunning [3s,2p] contraction of the Huzinaga (9s,5p) basis was used. We supplemented the nitrogen basis with polarization functions ($\alpha_d = 0.760$) [11].

Acknowledgement

We would like to thank Dr.P.J. Hay for the use of the molybdenum effective potential. The parameters of the potential are tabulated in table 7. We thank Professor Tom Dunn of Michigan State University for providing the experimental data and references in advance of publication [6]. Acknowledgement is made to the Donors of the Petroleum Research Fund, administered by the American Chemical Society, for the partial support of this research (Grant No. 13110-AC5,6).

References

[1] R.R. Schrock, J. Am. Chem. Soc. 96 (1974) 6796; 98 (1976) 5399;
R.R. Schrock and P.R. Sharp, J. Am. Chem. Soc. 100 (1978) 2389;
R.R. Schrock, S. Rocklage, J. Wengrovius, G. Rupprecht and J. Fellmann, J. Mol. Catal. 8 (1980) 73.
[2] A.K. Rappé and W.A. Goddard III, J. Am. Chem. Soc. 104 (1982) 448, 3287.
[3] E.L. Muetterties and E. Band, J. Am. Chem. Soc. 102 (1980) 6574.
[4] J. Chatt, J.R. Dilworth and R.L. Richards, Chem. Rev. 78 (1978) 589.
[5] R.K. Grasselli and J.D. Burrington, Advances in catalysis (Academic Press, New York, 1981) p. 133.
[6] R. Carlson, Ph.D. Thesis, Michigan State University (1982).
[7] C.W. Wilson Jr. and W.A. Goddard III, Chem. Phys. Letters 5 (1970) 45.
[8] C.E. Moore, Nat. Stand. Ref. Data Ser., Nat. Bur. Stand. (US), NSRDS-NBS 35, Vol. 3 (US Govt. Printing Office, Washington, 1971).
[9] L.G. Yaffe and W.A. Goddard III, Phys. Rev. A 13 (1976) 1682;
M.M. Goodgame and W.A. Goddard III, to be published
[10] P.J. Hay, private communication.
[11] R.A. Bair and W.A. Goddard III, J. Phys. Chem., submitted for publication.